Supporting Information

Duan et al. 10.1073/pnas.1005366107

SI Materials and Methods

Plant Growth and Plant and Protoplast Transformation. *Arabidopsis* seeds were surface sterilized and germinated on B5 medium supplemented with 1% sucrose and solidified by 0.7% agar. Seeds were cold treated at 4 °C for 2 d for synchronization before transferring to 22 °C for germination. When supplemented with auxin, 1-naphthaleneacetic acid (NAA) was added to concentrations indicated in the figures. For growth to maturity, 10-d-old seedlings were transferred to soil and maintained in a growth chamber at 22 °C under 16/8 h light/dark cycles. *Arabidopsis* was transformed by floral dip (1) and transgenic plants were selected on kanamycin-containing (50 μg/mL) medium. Mesophyll and root protoplasts were isolated from 3-wk-old seedlings or root tissues of 2- to 3-wk-old plants grown vertically in tissue culture, respectively. Protoplast transformation followed previously described procedures (2).

Molecular, Biochemical, and Histochemical Analysis. All recombinant DNA procedures were performed according to standard and PCR-based methodology. Table S1 shows a lists of primers used for cloning of cDNAs and genomic fragments and PCR amplification. Basic cloning strategies were used; sequences compatible with restriction enzyme recognition sites were included at the end of primers shown in Table S1, indicating cloning strategies. *FER* promoter (p*FER*)::*FER*-GFP containing 2,007 bp upstream of the FER coding region was cloned in *Agrobacterium* Ti plasmid intermediate vector pAC1352 (3), introduced into *Agrobacterium* GV2260 (4) and used to transform wild type (WT), *fer-4*, and *fer-5*. CaMV35S–FER–GFP, GFP–ROP2 (5), and NtRAC1(CA) (2) were similarly transformed into WT and *fer* plants as indicated in the text. p*FER*::GUS was derived from pBI121 (Clontech) and transformed into WT *Arabidopsis*. Plasmids used in protoplast transient transfection assays, 35S–FER–HA and 35S–ROPGEF4–HA were constructed in Bluescript pSK (Strategene) using full-length FER and ROPGEF1 cDNAs. ICR1–MBP and ROP2–MBP were derived from pMALC (NEB) for *Escherichia coli* expression. Genomic DNA was used for PCR analysis of T-DNA inserts. RNA from 10-d-old seedlings isolated by the PrepEase RNA isolation kit (USB/Affymetrix) was used in RT-PCR analysis for gene expression. The Clontech MATCHMAKER 2 protocol was used for yeast two-hybrid assays (6). ROPGEF1 cDNA was cloned into the BD vector described in ref. 7 except that the gene for ampicillin resistance was replaced by NPTII to facilitate subsequent recovery of kanamycin-resistant plasmids in *E. coli*. The kinase domain of FER was tested both as fusion with BD and AD with GEF1–AD and GEF1–BD, accordingly. GUS staining of transgenic seedlings followed standard procedure (8) in 0.2 mg/mL X-gluc at 37 °C for 16 h.

Microscopy. Fluorescence and DIC microscopy were carried out on a NIKON Eclipse E800 microscope equipped with a SPOT camera (Molecular Diagnostic). In comparative studies, image acquisition conditions are detailed in the figure legends. An Olympus SZ61 dissection microscope with a Q imaging camera was used to acquire seedling, inflorescence, and trichome images.

Pulldown Assays. For ICR1 and PBD pulldown of activated RAC/ROPs, ICR1–MBP, and PBD–GST (2) was expressed in *E. coli* BL21 by IPTG (0.5 mM) induction. Cells were resuspended in binding buffer [40 mM Tris-HCl (pH 7.5), 100 mM NaCl, 1 mM Na_2-EDTA] and sonicated (six 10-s pulses at 1-min intervals) for protein extraction. After removal of cell debris by centrifugation at 4 °C, proteins were applied to amylose resin (NEB) or GST resin in the same buffer and the ICR1–MBP or PBD–GST-bound resin was used to pull down activated RAC/ROPs. For target proteins, the roots of 7-d-old WT and *fer-4*, *-5* seedlings were homogenized in liquid N_2 and 100 mg of frozen powder was extracted in pulldown buffer [binding buffer, plus 5% glycerol, 1 mM PMSF, protease inhibitor mixture (Calbiochem)] supplemented with 0.75% Triton X-100. Proteins were extracted at 4 °C with mixing for 15 min. The debris was removed by centrifugation at top speed in a microcentrifuge for 10 min at 4 °C. A total of 90% of the supernatant was applied to the ICR1–MBP-bound or PBD–GST-bound resin for pulldown assays. The remaining 10% of the supernatant was saved for protein quantification. Pulldown was carried out by binding extracted proteins to the amylose resin at 4 °C for 2 h. The resin was washed five times in binding buffer. Proteins remained bound to the resin were eluted in SDS/PAGE loading buffer, boiled for 5 min, and applied to 15% SDS/PAGE for protein blot analysis. Protein blots were stained by Ponçeau Red to ensure comparable loading of samples. RAC/ROP detection was carried out by binding with anti-NtRac1 antibodies (2), followed by horseradish peroxidase-conjugated secondary antibodies and chemiluminescence detection (for ICR–MBP pulldown) or alkaline phosphatase-conjugated secondary antibodies and colorimetric detection (for PBP–GST pulldown). Data from immunoblot were quantified by Adobe Photoshop. Mean histogram values were quantified for ROIs of identical area from each band after background subtraction from blank region of the blots.

For ROP2 pulldown of FER and GEF4–HA, ROP2–MBP-bound amylose resin was generated as described above. For protoplast-expressed FER and GEF4, mesophyll or root protoplasts were transfected by 5–10 μg CaMV35S::FER-HA or CaMV35S::GEF4-HA. After overnight culture, protoplasts were collected and sonicated in pulldown buffer. After sonication, Triton X-100 was added to the extract to a final concentration of 0.4%, followed by 15 min. of shaking at 4 °C. Pulldown reactions and subsequent analyses were as described above. Five-day-old p*FER*–FER–GFP seedlings were also used for ROP2–MBP pulldown analysis. Seedlings were ground in liquid nitrogen and resuspended in extraction buffer [40 mM Tris-HCl (pH 7.5), 100 mM NaCl, 5% glycerol, 1 mM Na_2-EDTA, PMSF, and protease inhibitor mixture (Calbiochem)]. Microsomes were extracted at 4 °C with mixing for 30 min. Cell debris was removed by centrifugation at 10,000 *g* at 4 °C and the resulting supernatant was centrifuged at 100,000 *g* for 3 h to pellet the microsomal fraction. The pellet was resuspended in extraction buffer supplemented with 0.3% Triton X-100 and then centrifuged again at 2,000 *g* to remove insoluble material. The microsomal extract was then used for pulldown analysis. HA antibody (Santa Cruz) was used for detection.

Mutant Screening. One to three T-DNA insertion mutants for several vegetative tissue-expressed FER-related genes, At2g23200 (HERK4), At5g24010 (HERK5), At5g54380 (THE1), At3g46290 (HERK1), At5g61350, At3g51550 (FER), At1g30570 (HERK2), At2g39360 (HERK3), At5g39000, At5g38990, At5g39030, and At5g39020 were obtained from the Salk collection and screened for root hair defects in 3- to 4-d-old seedlings. Only insertions in At3g51550 (FER) induced readily noticeable root hair defects and were studied in detail. The bulk of the screening was carried out in 2007 and should be considered preliminary.

Statistics. Fig. 3*B* shows the difference between WT and *fer-5* was significant, $P < 0.05$, 10^{-4}, 10^{-4} at 0, 50, and 100 nM NAA.

Difference between WT and complemented *fer-5* was insignificant under all conditions ($P > 0.1$). Difference between untreated and NAA treated *fer-5* was insignificant ($P > 0.05$).

Fig. 3*C* shows the difference between WT and *fer-4* was significant, $P < 10^{-4}$ at 0 and 100 nM NAA. Difference between untreated and NAA-treated WT was significant ($P < 10^{-6}$). Difference between untreated and NAA-treated *fer-4* was insignificant ($P \geq 0.5$).

Fig. 3*E* shows the difference between WT and *fer-5* was significant, $P < 0.05$, 10^{-4}, 10^{-4} at 0, 50, 100 nM NAA. Difference between WT and ROP2-rescued *fer-5* was insignificant under all conditions ($P > 0.1$). Difference between untreated and NAA-treated *fer-5* was insignificant ($P > 0.05$). Difference between untreated and NAA-treated GFP–ROP2-rescued *fer-5* was significant ($P < 10^{-4}$).

Fig. 4 *E* and *G* shows the difference between WT and *fer-4, -5* and *srn* was significant ($P < 10^{-6}$) under both conditions. Difference between untreated and NAA-treated WT was significant ($P < 10^{-5}$). Difference between untreated and NAA-treated *fer-4, srn* was insignificant ($P > 0.05$), but significant for *fer-5* ($P < 0.05$), reflecting a weaker phenotype than the two null mutants.

Fig. 4*I* shows the difference between WT and mutants was significant ($P < 10^{-6}$), between WT and complemented mutants was insignificant ($P > 0.1$).

Fig. 5*B* shows the difference was significant ($P < 10^{-4}$) between WT and *fer-5*, insignificant ($P > 0.1$) between WT and GFP–ROP2-rescued *fer-5*, and significant ($P < 10^{-2}$) between *fer-5* and GFP–ROP2-rescued *fer-5*. Note signal in GFP–ROP2-rescued *fer-5* without incubation with the ROS substrate H_2DCFDA (fourth data bar) was negligible.

1. Clough SJ, Bent AF (1998) Floral dip: A simplified method for *Agrobacterium*-mediated transformation of Arabidopsis thaliana. *Plant J* 16:735–743.
2. Tao LZ, Cheung AY, Wu HM (2002) Plant Rac-like GTPases are activated by auxin and mediate auxin-responsive gene expression. *Plant Cell* 14:2745–2760.
3. Rodermel SR, Abbott MS, Bogorad L (1988) Nuclear-organelle interactions: Nuclear antisense gene inhibits ribulose bisphosphate carboxylase enzyme levels in transformed tobacco plants. *Cell* 55:673–681.
4. Deblaere R, et al. (1985) Efficient octopine Ti plasmid-derived vectors for Agrobacterium-mediated gene transfer to plants. *Nucleic Acids Res* 13:4777–4788.
5. Jones MA, Raymond MJ, Yang Z, Smirnoff N (2007) NADPH oxidase-dependent reactive oxygen species formation required for root hair growth depends on ROP GTPase. *J Exp Bot* 58:1261–1270.
6. Gietz D, St Jean A, Woods RA, Schiestl RH (1992) Improved method for high efficiency transformation of intact yeast cells. *Nucleic Acids Res* 20:1425.
7. James P, Halladay J, Craig EA (1996) Genomic libraries and a host strain designed for highly efficient two-hybrid selection in yeast. *Genetics* 114:1425–1436.
8. Jefferson RA, Kavanagh TA, Bevan MW (1987) GUS fusions: β-Glucuronidase as a sensitive and versatile gene fusion marker in higher plants. *EMBO J* 6:3901–3907.
9. Lavy M, et al. (2007) A novel ROP/RAC effector links cell polarity, root-meristem maintenance, and vesicle trafficking. *Curr Biol* 17:947–952.
10. Nibau C, Wu H-M, Cheung AY (2006) RAC/ROP GTPases: 'Hubs' for signal integration and diversification in plants. *Trends Plant Sci* 11:309–315.
11. Yang Z, Fu Y (2007) ROP/RAC GTPase signaling. *Curr Opin Plant Biol* 10:490–494.
12. Carol RJ, Dolan L (2006) The role of reactive oxygen species in cell growth: Lessons from root hairs. *J Exp Bot* 57:1829–1834.
13. Swanson S, Gilroy S (2010) ROS in plant development. *Physiol Plant* 138:384–392.
14. Jaspers P, Kangasjärvi J (2010) Reactive oxygen species in abiotic stress signaling. *Physiol Plant* 138:405–413.
15. Torres MA (2010) ROS in biotic interactions. *Physiol Plant* 138:414–429.
16. Wong HL, et al. (2007) Regulation of rice NADPH oxidase by binding of Rac GTPase to its N-terminal extension. *Plant Cell* 19:4022–4034.
17. Kaothien P, et al. (2005) Kinase partner protein interacts with the LePRK1 and LePRK2 receptor kinases and plays a role in polarized pollen tube growth. *Plant J* 42:492–503.
18. Zhang Y, McCormick S (2007) A distinct mechanism regulating a pollen-specific guanine nucleotide exchange factor for the small GTPase Rop in *Arabidopsis thaliana*. *Proc Natl Acad Sci USA* 104:18830–18835.
19. Lemichez E, et al. (2001) Inactivation of AtRac1 by abscisic acid is essential for stomatal closure. *Genes Dev* 15:1808–1816.
20. Foreman J, et al. (2003) Reactive oxygen species produced by NADPH oxidase regulate plant cell growth. *Nature* 422:442–446.
21. Carol RJ, et al. (2005) A RhoGDP dissociation inhibitor spatially regulates growth in root hair cells. *Nature* 438:1013–1016.
22. Berken A, Thomas C, Wittinghofer A (2005) A new family of RhoGEFs activates the Rop molecular switch in plants. *Nature* 436:1176–1180.
23. Gu Y, Li S, Lord EM, Yang Z (2006) Members of a novel class of Arabidopsis Rho guanine nucleotide exchange factors control Rho GTPase-dependent polar growth. *Plant Cell* 18:366–381.

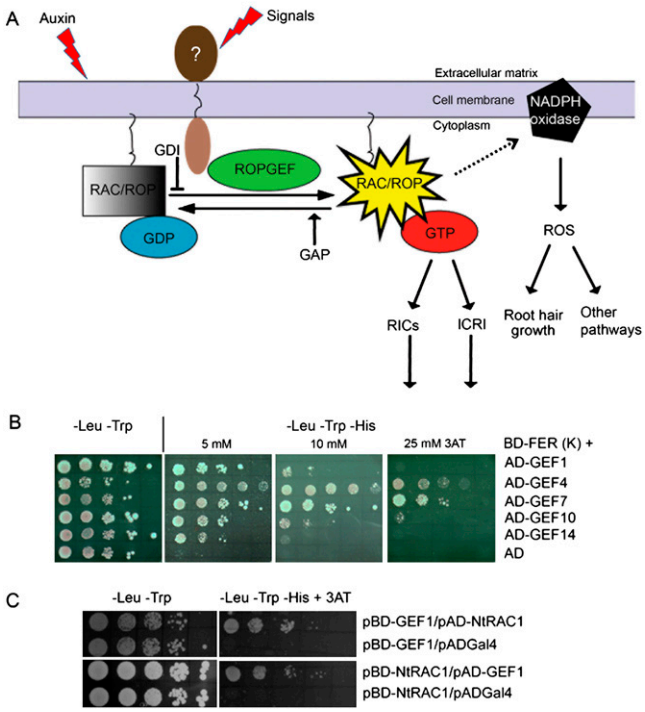

Fig. S1. (*A*) Schematic summary of the RAC/ROP signaling pathway showing the key elements involved in this study. ROPGEFs stimulate GDP/GTP exchange to activate RAC/ROPs. GDI and GAP (GTPase activating protein) are negative regulators, one inhibiting GDP dissociation and the other accelerating GTP hydrolysis, respectively (10). Activated RAC/ROPs interact directly with downstream effectors RICs and ICR1 to mediate diverse cellular pathways (9–11). RAC/ROP-mediated NADPH-oxidase–dependent ROS production is well established in mediating root hair growth and several biotic and abiotic stress-induced responses (12–16). In rice, NADPH oxidase has also been shown to be an immediate effector for OsRac1 to mediate pathogen-elicited defense responses (16). A large number of surface regulators (designated as ? in the figure) may be involved in mediating diverse signals to RAC/ROP-regulated pathways, but only two are known (17, 18). Hormones, such as auxin (2) and ABA (19) and pathogen elicitors (16) have been shown to regulate RAC/ROP signaling. Using a ROPGEF as a molecular link, we report here identification of a surface regulator, FER, for the RAC/ROP-regulated pathway that stimulates NADPH oxidase-dependent ROS production to mediate polarized root hair growth (20, 21). (*B*) Yeast two-hybrid assays showing FER kinase domain [FER(K)] interact with multiple *Arabidopsis* ROPGEFs. The originally isolated ROPGEF1-interacting fragments spanned half the RLKs' kinase domain till the end of their coding region. (*C*) Yeast two-hybrid assays showing ROPGEF1 interact with NtRAC1 (2), similar to previously shown for ROPGEFs and RAC/ROPs from *Arabidopsis* (22, 23).

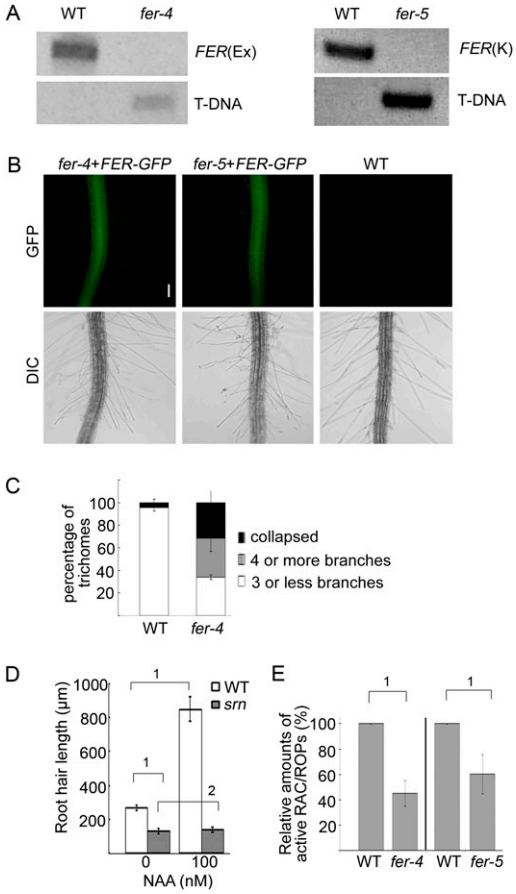

Fig. S2. Additional characterization of *fer* and complemented *fer* mutants. (*A*) Genomic DNA PCR analysis for *fer-4* and *fer-5*. T-DNA insert was present in the *fer* mutants but not in WT (T-DNA) and genomic FER DNA fragments were present in WT but not in *fer* mutants [FER(Ex) and FER(K)]. For *fer-4*, primers 1 and GABI(R) were used for the T-DNA insert and primers 1 and 2 were used for the WT FER DNA fragments; for *fer-5*, primers 3 and LB1 and primers 3 and 4 were used, respectively. See Fig. 2*A* and *SI Materials and Methods* for primer information. (*B*) FER–GFP expression in p*FER*::*FER-GFP* transformed *fer-4* and *fer-5* mutants correlated with complemented root hair phenotype. (Scale bar, 100 μm.) (*C*) Quantitative data for *fer-4*–induced trichome defects. Data show the mean % of each category of trichomes averaged from four comparably aged true leaves from 3-wk-old seedlings (a total of ~350 trichomes were counted per sample). Differences between WT and *fer-4* are significant, Student's *t*-tests showed $P < 10^{-7}$ for trichomes with three or fewer branches, $P = 1.15 \times 10^{-3}$ for those with more than four branches, and $P = 4.7 \times 10^{-3}$ for collapsed trichomes. (*D*) Root hair length comparison between WT and *srn*. Root hair lengths shown for *srn* were overestimations because only hairs with measurable lengths but not the most severe ones that never elongated were included in the data set. (*E*) Relative levels of ROP–MBP pulled down *fer-4* and ROP–GST pulled down *fer-5*. Data were averaged from quantification of data obtained from three independent experiments. 1, significant difference ($P < 0.05$); 2, insignificant difference ($P > 0.05$).

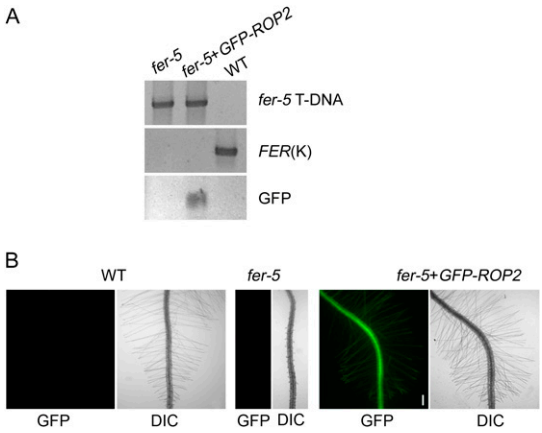

Fig. S3. Analysis of *CaMV35S*::*GFP-ROP2* transformed *fer-5*. (*A*) Genomic PCR analysis confirms presence of the original T-DNA insert (*fer-5* T-DNA) using primers LB1 and 3 (see Fig. 2*A*), absence of the WT *FER* [*FER*(K)] using primers 3 and 4, confirming homozgyosity of the T-DNA insertion locus, and presence of GFP DNA in the *CaMV35S*::*GFP-ROP2* transformed *fer-5*. (*B*) Root hairs in *fer-5* were restored to normal in GFP–ROP2-expressing *CaMV35S*::*GFP-ROP2* transformed *fer-5*. (Scale bar, 200 μm.)

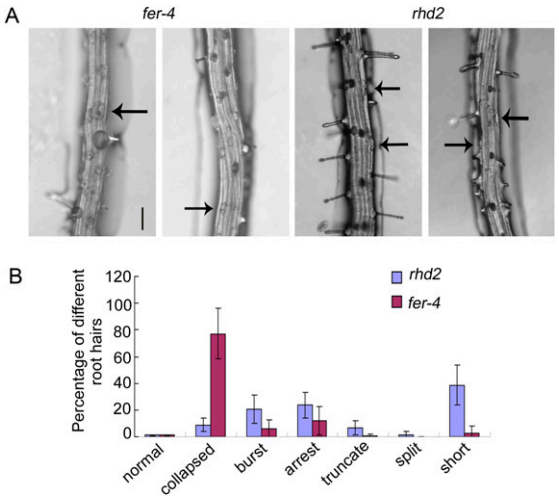

Fig. S4. Comparison of root hair phenotypes in *fer-4* and *rhd2*. (*A*) Root segments from 4-d-old *fer-4* and *rhd2* mutant seedlings. Arrows point to collapsed root hairs. (Scale bar, 100 μm.) (*B*) Quantitative comparison of root hair defects. Data show that collapsed root hairs predominated in *fer-4*, whereas *rhd2* root hair defects were more broadly distributed among different severity classes (see Fig. 2*D* for definition), indicating *fer-4* induced more severely defective root hairs. Each data bar represents the mean ± SD where n = 600 root hairs sampled from 12 four-day-old seedlings.

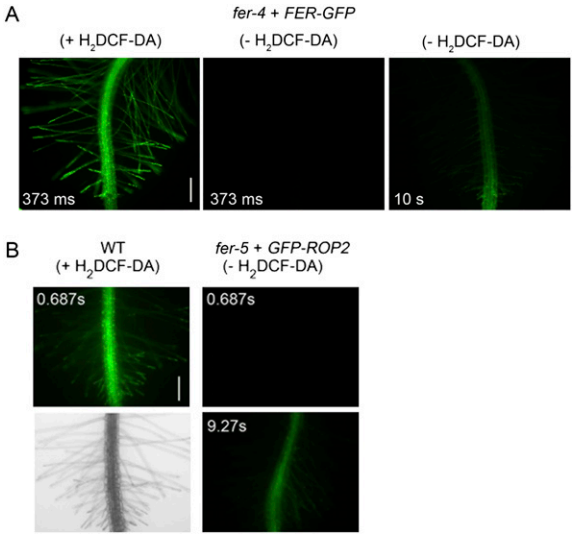

Fig. S5. GFP signal from p*FER*::*FER-GFP* and *CaMV35S*::*GFP-ROP2*–transformed *fer* seedlings was negligible under H_2DCF–DA-detected ROS imaging condition. (*A*) p*FER*::*FER-GFP* transformed *fer-4* seedlings observed with (+) or without (–) H_2DCF–DA treatment. The + H_2DCF–DA image was acquired by autoexposure (373 ms); when exposed under the same condition, GFP signal from the – H_2DCF–DA seedling was not detectable. Autoexposure of the same – H_2DCF–DA seedling required a 10-s exposure, suggesting FER–GFP signal could not interfere with ROS detection. (*B*) *CaMV35S*::*GFP-ROP2* transformed *fer-5* seedlings observed with (+) or without (–) H_2DCF–DA treatment. (*Left*) The WT seedling was treated with H_2DCF–DA for ROS analysis and imaged by autoexposure (*Upper*; exposure time was 0.687 s). *Lower* panel shows a DIC image of the WT seedling. (*Right*) The *fer-5* + *GFP–ROP2* seedling was not treated for ROS detection and imaged using 0.687-s exposure time (*Upper*) to detect contribution to the fluorescence signal by GFP–ROP2, which was negligible. *Lower* panel shows an autoexposed image of the same *fer-5* + GFP–ROP2 seedling root to reveal the GFP signal. The long autoexposure time (9.27 s) signified a very low fluorescence level from GFP–ROP2 under ROS detection condition.

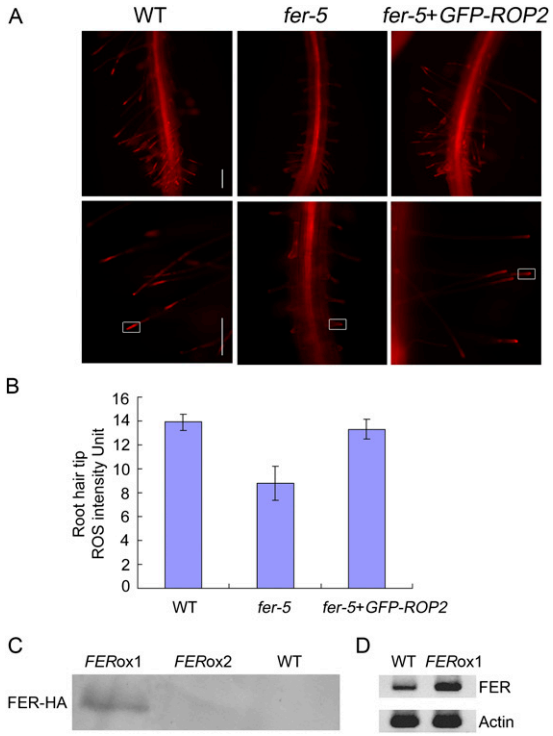

Fig. S6. (*A* and *B*) Dihydroethidium (DHE) detection of ROS shows strong signals in WT (*Left*) and CaMV35S::GFP-ROP2–rescued *fer-5* (*Right*), whose root hairs showed normal growth, but not in *fer-5* mutant, whose root hairs showed aborted growth (*Middle*). *Lower* panels show higher magnification images acquired using the WT imaging condition for quantification of signals at root hair tips in boxed ROIs of identical areas. (*B*) Average ROS level (n = 43 root hairs per sample) quantified from ROI of identical areas (boxes in *A*). Difference was significant ($P < 0.05$) between WT and *fer-5*, between *fer-5* and GFP–ROP2-rescued *fer-5*, and insignificant ($P > 0.05$) between WT and GFP–ROPs-rescued *fer-5*. (*C*) Protein blot analysis for CaMV35S::FER-HA overexpression lines. FERox1 was representative of lines with detectable FER–HA and showed enhanced root ROS accumulation relative to WT (see Fig.5 *C* and *D*). FERox2 was representative of the majority of similarly transformed lines; they did not accumulate detectable levels of FER–HA and their ROS levels were not distinguishable from controls. We could not recover transgenic lines expressing levels of FER–HA higher than that observed in FERox1. (*D*) RT-PCR for FER mRNA levels in WT and *FER*ox1 seedlings (7 d). Primers 1 and 2 (see Fig. 2*A*) were used for FER DNA amplification.

Table S1. List of primers

cDNA/genomic DNA	Primers (top row forward; bottom row reverse)	RE* site
	Primers used for cloning purposes	
FER cDNA	CGGATCCATGAAGATCACAGAGGGACGATTC	BamHI/EcoRI
	CGAATTCACGTCCCTTTGGATTCATGATCTG	
GEF1 cDNA	GAGATCTATGGGGAGCTTATCTTC	BglII/NcoI
	CCCATGGCATCTCTTTCCGGCGTCACTCC	
GEF4 cDNA	CGGATCCATGGAGAGTTCTTCGAATTCC	BamHI/NcoI
	GCCATGGCATCATCTCTGTTTCTCACTG	
FER promoter	CGCGGCCGCCGAGTTGTAAAAGGCCTGGCTAAAG	NotI/BamHI
	CGGATCCCGATCAAGAGCACTTCTCCGGG	
ICR1 cDNA	CAGATCTATGCCAAGACCAAGAGTTTCAGAG	BglII/EcoRI
	CGAATTCCTTTTGCCCTTTCTTCCTCCAC	
ROP2 cDNA	CGGATCCATGGCGTCAAGGTTTATTAAG	BamHI/SalI
	CGTCGACTCACAAGAACGCGCAACGGTTC	
	Primers used for PCR analysis	
Primer 1†	CGGATCCATGAAGATCACAGAGGGACGATTC	
Primer 2†	CGCAGATCTAGCACCAAACACACAAAACCC	
Primer 3†	CGGATCCATGGCTTACCGCAGACGTAAGCGTGG	
Primer 4†	CGAATTCACGTCCCTTTGGATTCATCATCTG	
LB1†	GCGTGGACCGCTTGCTGCAACT	
GAB1 (R)†	GTGGATTGATGTGATATCTCC	
GFP	CGGATCCATGGTGAGCAAGGGCGAGGAG	
	CGTCGACTTACTTGTACAGCTCGTCCATGCC	
Actin2	CGTACAACCGGTATTGTGCTGG	
	GGAGATCCACATCTGCTGGAATG	

*Restriction enzyme.
†See Fig. 2 for primer designation.